

## SMALL/MEDIUM-ANGLE DIFFRACTOMETER WINK

M. Furusaka, K. Suzuya, N. Watanabe, \*M. Osawa, I. Fujikawa and S. Satoh

National Laboratory for High Energy Physics, Tsukuba 305

\*Institute of Materials Science, University of Tsukuba, Tsukuba 305

### Abstract

WINK is a special instrument which covers very wide momentum transfer range ( $0.01 \leq Q \leq 20 \text{ \AA}^{-1}$ ) by using incident neutrons of wide wavelength band ( $1 < \lambda < 16 \text{ \AA}$ ), together with wide scattering-angle coverage ( $2^\circ \leq \theta \leq 145^\circ$ ). To show the capabilities of WINK, we performed measurements of SiC fibers which have very complex mesoscopic structures. We also performed conventional X-ray small-angle and wide-angle diffraction to compliment the analyses. WINK was proved to be a very powerful instrument to analyze such complex materials; i) concentrations of hydrogen atoms were determined from incoherent scattering intensity at around  $Q = 1 \text{ \AA}^{-1}$ , ii) voids as little as  $4 \text{ \AA}$  in diameter were observed, iii) the size of  $\beta$ -SiC obtained by SANS was different from that by diffraction at high angle, iv) glassy carbon and vitreous silica were detected in the power scattering.

### Introduction

WINK is a special instrument which is a combination of a small-angle instrument, a medium-resolution powder diffractometer and a total-scattering instrument. It is designed for characterization of various materials which have mesoscopic scale structures, like biology samples, micelles and emulsions, membranes, polymers, "hard" materials, magnetic materials and so on. To show the capabilities of WINK, we performed measurements on SiC-fibers, and detailed structure analysis was done. SiC-fiber is a material which has very high tensile strength even at high temperature. As common in such materials, it shows very complex mesoscopic structures<sup>1)</sup>; it is not a homogeneous system and consists of several components and phases.

This study is also a good example of using both X-ray (SAXS) and neutron (SANS) small-angle scattering method to analyze very complex structure; the differences in the scattering amplitude density for both probe between the components are significant in this sample.

### Current status of WINK

Fig. 1 shows a side view of WINK. Design specifications of WINK are described elsewhere<sup>2)</sup>. Last two years, we focused our effort to establish how to analyze data taken by WINK, since the use of such wide incoming neutron wavelength band together with wide scattering angle range has never been realized. For example, we found a deviation from Maxwellian distribution above  $12 \text{ \AA}$  in incident neutron spectrum. We also found that we could distinguish frame overlapped scattering by comparing scattering in the same  $Q$  bin obtained from different detector at different angle and wavelength. Therefore, there is no need for a frame-overlap eliminating chopper.

For the hardware side, we now have nearly 100 conventional  $^3\text{He}$  detectors working, mainly in a small-angle detector bank. We will have additional 40 detectors working in a 1.1m detector bank by the end of this fiscal year. We still have tentative setup for a higher-angle detector bank which surrounds the sample position.

### Sample preparation

SiC fibers were produced from Polycarbosilane ( $\text{Si}_{1.93}\text{CH}_{4.71}\text{O}_{0.01}$ ). The first step for making commercial SiC fibers (Si-C-O fibers) are a thermal oxidation curing process to make

bridges between microscopic fibers. However, oxygen introduced into the fibers by the curing process causes a drastic thermal degradation of the fibers. Electron beam irradiation is a good alternative to the curing process, and it can produce oxygen-free SiC fibers<sup>2)</sup> (Si-C fibers). Following these curing processes, the samples are heat treated at various high temperatures (heat treatment temperature: HTT). We studied samples prepared by the above two curing processes, at the HTT's of 1273K, 1473K, and 1673K for each case.

## Results and Discussions

First, residual hydrogen contents were determined from the scattering at medium-Q range, as shown by the line denoted by  $I_{inc}^N$  in Fig. 2, where coherent cross-section is negligible. We assumed that incoherent scattering from hydrogen atoms is the only contribution to the scattering in such a Q range. The hydrogen contents thus obtained were in good agreement with that from chemical analysis. Because of the large incoherent cross-section of the hydrogen atom, sensitivity is very high for the neutron scattering.

In the case of small-angle scattering, neutron (SANS) and X-ray (SAXS) scattering looks quite different at a first glance, as shown in Fig. 2, especially at higher Q range ( $0.1 < Q < 1 \text{ \AA}^{-1}$ ), even after subtracting the incoherent scattering from hydrogen atoms.

SAXS shows  $I(Q) \sim Q^{-4}$  power law in the Q range  $0.1 < Q < 0.2 \text{ \AA}^{-1}$ , whereas, SANS has a shoulder at around  $Q = 0.3 \text{ \AA}^{-1}$ . Therefore, we assume that the SANS data consist of three components; a broad peak, a shoulder and a constant spectrum. Those components are expressed by the scattering functions  $I_1(Q)$ ,  $I_2(Q)$  and  $I_{inc}$ , respectively. The SAXS data should also consist of these functions, although such a shoulder and a constant spectrum are not observed distinctly in Fig. 2. Consequently, the neutron and X-ray scattering cross-sections can be expressed by the following equation:

$$\left[ \frac{d\Sigma}{d\Omega}(Q) \right]^{N,X} = C_1^{N,X} I_1^{N,X}(Q) + C_2^{N,X} I_2^{N,X}(Q) + I_{inc}^{N,X}, \quad (1)$$

where  $C_1$  and  $C_2$  are the coefficients, N and X refer to neutron and X-ray.

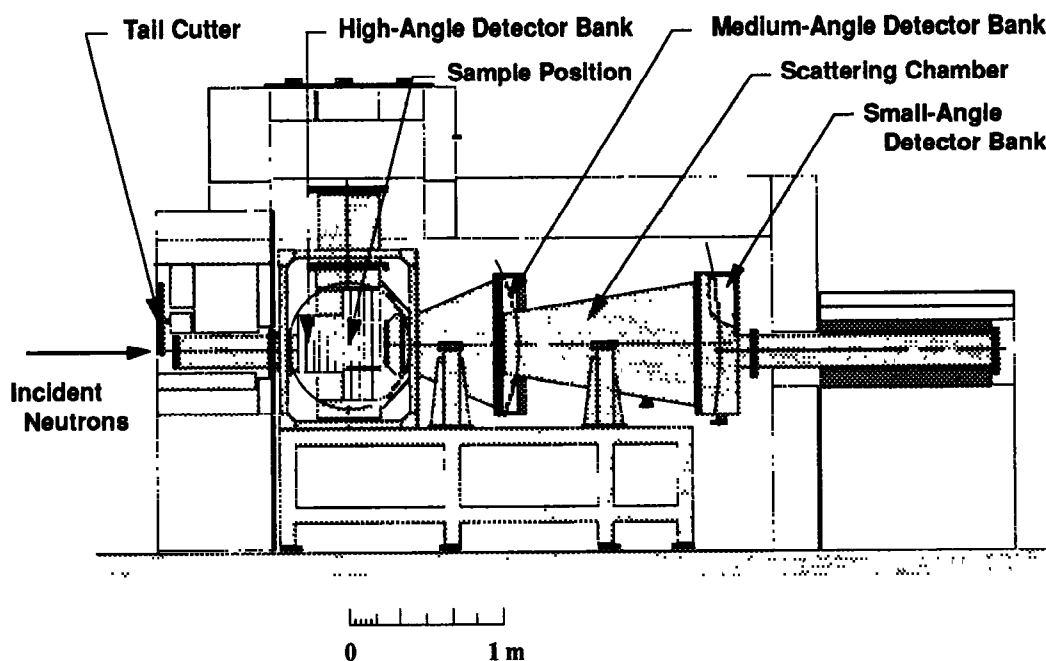


Fig. 1. Schematic diagram of WINK.

As a first step of the data analysis, we made the following assumptions; i)  $I_1(Q)$  obeys Porod law at high  $Q$  ( $0.1 \sim 0.2 \text{ \AA}^{-1}$ ) as obtained from the SAXS data, ii)  $I_2(Q)$  is represented by the Debye-Bueche formula. Therefore the scattering cross-section at high  $Q$  is expressed as follows:

$$\left[ \frac{d\Sigma}{d\Omega}(Q) \right]^{N,X} = C_1^{N,X} Q^{-4} + \frac{C_2^{N,X}}{(1+Q^2\xi^2)^2} + I_{inc}^{N,X}, \quad (2)$$

where  $\xi$  is a correlation length. First, we fitted high- $Q$  part of the SAXS data with equation 2, and obtained  $I_1^X(Q)$ . We then fitted SANS data assuming that the  $I_1^N(Q)$  has the same  $Q$  dependence as the  $I_1^X(Q)$  for the whole  $Q$  range. Since SANS has much more pronounced shoulder around  $Q \sim 0.3 \text{ \AA}^{-1}$ , we could determine the  $\xi$  in the second term of equation 2 more reliably than the SAXS data fitting. By using the same  $\xi$ , we fitted the SAXS data again using equation 2. Finally, we fit the SANS data using more reliable  $I_1^X(Q)$ . Figure 3 shows the result of the fitting to the SANS data.

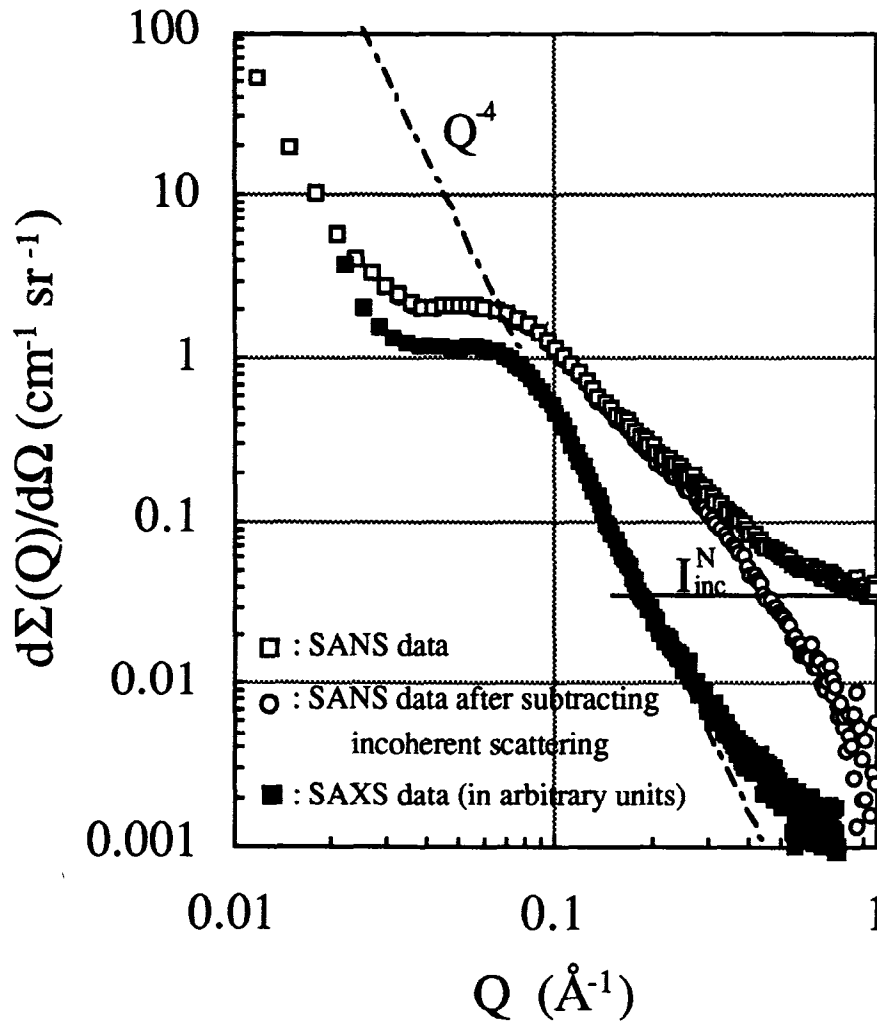


Fig. 2. SANS and SAXS data for SiC fibers (HTT=1473K).

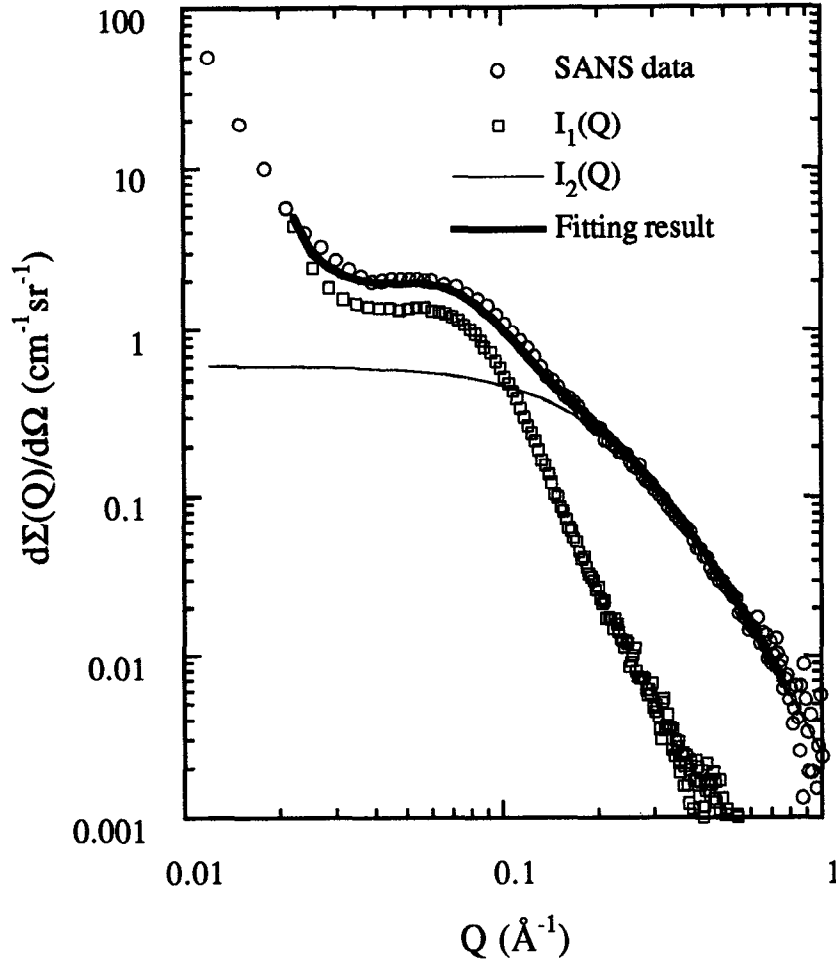


Fig. 3. Result of SANS data fitting for SiC fibers (HTT=1473K)

From macroscopic density measurements and chemical analysis, together with the results from the above fittings, we concluded that the SiC fibers consist of four basic phases;  $\beta$ -SiC( $I_1(Q)$ ), vitreous SiO<sub>2</sub>, glassy carbon and void( $I_2(Q)$ )<sup>1</sup>. Since the main component should be  $\beta$ -SiC, and void has higher contrast in SANS than in SAXS, the conclusion is quite natural.

The radius  $R_v$  of the voids were obtained from the  $\xi$ , using the following equation,

$$R_v = \frac{3\xi}{4(1 - \phi_{void})}, \quad (3)$$

where  $\phi_{void}$  is a volume fraction of the voids. The diameter of the voids thus obtained were from 4Å to 13Å, depending on the curing processes and HTT's. It is almost impossible to measure small voids of such size with other methods; we have to use incoming neutrons of long wavelengths which are longer than Bragg-cutoff to avoid multi-Bragg reflections, and simultaneously, have to cover up to relatively high  $Q$  to about 1Å<sup>-1</sup>. WINK was designed for this purpose and it was very good at measuring such things.

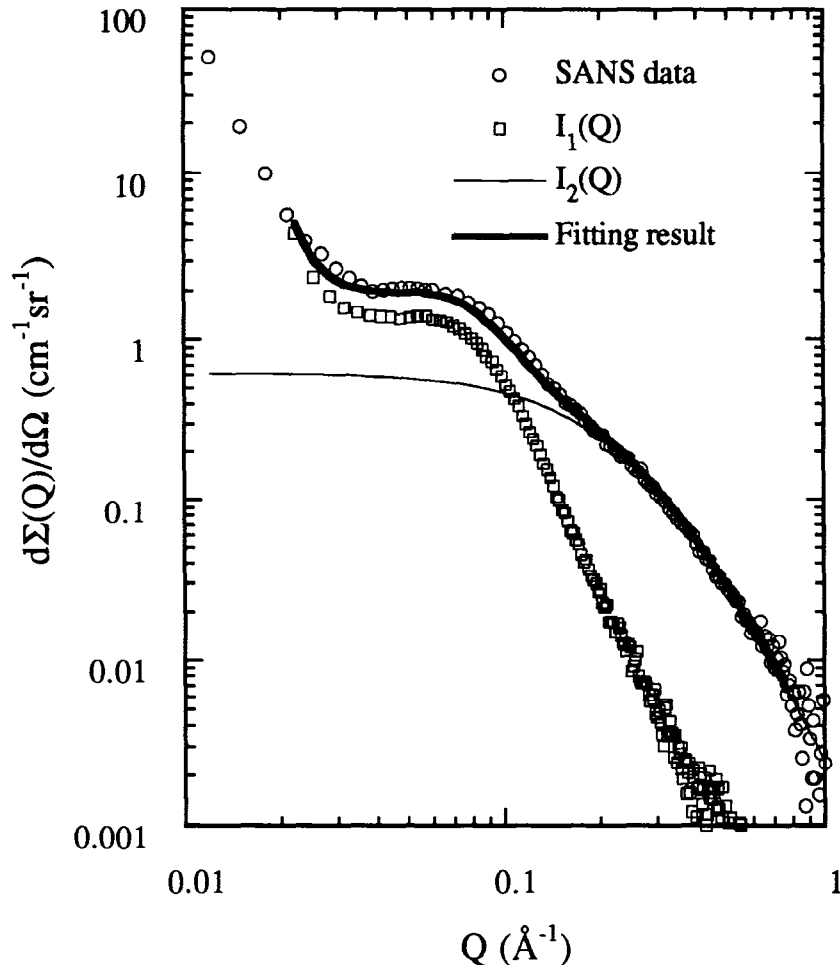


Fig. 4. Neutron diffraction patterns for Si-C and Si-C-O fibers (HTT=1473K).

We estimated the size of  $\beta$ -SiC crystallites  $L$  from the peak position of  $I_1^N(Q)$  and volume fraction of the  $\beta$ -SiC. We also determined the size  $D$  from a diffraction peak width obtained from the high-angle neutron (see Fig. 4) or X-ray diffraction using Scherrer equation,

$$D = \frac{0.9\lambda}{W \cos \theta}, \quad (4)$$

where  $\lambda$  is the wavelength of the incident neutrons or X-ray,  $W$  the full-width at half maximum (FWHM) of a Bragg peak and  $\theta$  the Bragg angle. Fig. 5 shows both  $L$  and  $D$  as a function of HTT. It is note worthy that the size of the crystallites observed by small-angle scattering  $L$  was much bigger than that obtained from the powder diffraction  $D$ . The size observed by the small-angle scattering did not reflect the size of a single crystallite, but it is a measure of a particle which consists of small crystallites which were observed by the powder diffraction.

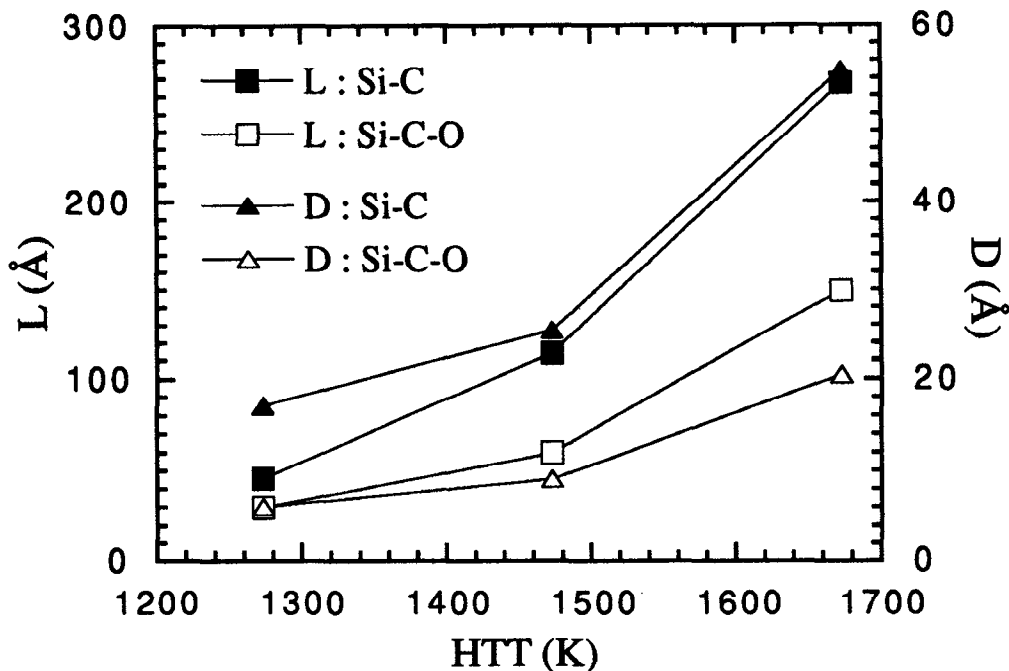


Fig. 5. Sizes of particles L and crystallites D of  $\beta$ -SiC.

Figure 4 shows diffraction patterns from SiC fibers. Besides the powder diffraction from  $\beta$ -SiC particles, small diffuse peaks were observed. We made a separate measurement for vitreous carbon, and plotted on the same figure. We scaled it by the peak around  $1.7\text{\AA}^{-1}$  of the glassy carbon to the diffraction pattern. The figure shows that not only could we reproduce the first peak, peaks around 3 and  $5.2\text{\AA}^{-1}$  were also attributed to the vitreous carbon. We also performed measurement on vitreous silica, and plotted on the bottom half of the Fig. 4. This time, the peak around  $1.5\text{\AA}^{-1}$  has different shape from Si-C fibers, and again it was well reproduced by the combination of vitreous silica and glassy carbon. In principle, we will be able to do a total fitting to multi-phase powder pattern and to total scattering simultaneously.

### Conclusions

We performed measurements on two kinds of SiC fibers using WINK and conventional SAXS and X-ray diffraction. WINK was proved to be a very powerful instrument to analyze such a complex material, especially when combined with X-ray diffraction.

### References

1. K. Suzuya, M. Furusaka, N. Watanabe, M. Osawa, K. Okamura, T. Kamiyama and K. Suzuki; submitted to J Am. Ceram. Soc.
2. M. Furusaka, N. Watanabe, K. Suzuya, I. Fujikawa and S. Satoh; ICANS-XI International Collaboration on Advanced Neutron Sources (KEK, Tsukuba, Oct. 22-26, 1990) P. 677.